

This is the accepted manuscript made available via CHORUS. The article has been published as:

Origin of Bardeen-Zumino current in lattice models of Weyl semimetals

E. V. Gorbar, V. A. Miransky, I. A. Shovkovy, and P. O. Sukhachov

Phys. Rev. B **96**, 085130 — Published 22 August 2017

DOI: [10.1103/PhysRevB.96.085130](https://doi.org/10.1103/PhysRevB.96.085130)

Origin of the Bardeen-Zumino current in lattice models of Weyl semimetals

E. V. Gorbar,^{1,2} V. A. Miransky,³ I. A. Shovkovy,^{4,5} and P. O. Sukhachov³

¹*Department of Physics, Taras Shevchenko National Kiev University, Kiev, 03680, Ukraine*

²*Bogolyubov Institute for Theoretical Physics, Kiev, 03680, Ukraine*

³*Department of Applied Mathematics, Western University, London, Ontario, Canada N6A 5B7*

⁴*College of Integrative Sciences and Arts, Arizona State University, Mesa, Arizona 85212, USA*

⁵*Department of Physics, Arizona State University, Tempe, Arizona 85287, USA*

For a generic lattice Hamiltonian of the electron states in Weyl semimetals, we calculate the electric charge and current densities in the first order in background electromagnetic and strain-induced pseudoelectromagnetic fields. We show that the resulting expressions for the densities contain contributions of two types. The contributions of the first type coincide with those in the chiral kinetic theory. The contributions of the second type contain the information about the whole Brillouin zone and cannot be reproduced in the chiral kinetic theory. Remarkably, the latter coincide exactly with the Bardeen-Zumino terms that are usually introduced in relativistic quantum field theory in order to define the consistent anomaly. We demonstrate the topological origin of the Bardeen-Zumino (or, equivalently, Chern-Simons) corrections by expressing them in terms of the winding number in the lattice Hamiltonian model.

I. INTRODUCTION

The possibility to observe the signatures of the chiral anomaly is one of the most intriguing aspects of the physics of Weyl semimetals, whose low-energy quasiparticles are described by the corresponding relativistic-like equation in the vicinity of Weyl nodes. A condensed-matter realization of Weyl fermions was first predicted theoretically in pyrochlore iridates [1]. Later, a number of materials (e.g., TaAs, TaP, NbAs, NbP, $\text{Mo}_x\text{W}_{1-x}\text{Te}$, and YbMnBi_2) were discovered to be Weyl semimetals [2–9]. In accordance with the general arguments of Nielsen and Ninomiya [10], Weyl nodes in such condensed-matter materials come in pairs of opposite chirality. In fact, typical Weyl semimetals have multiple pairs of opposite-chirality nodes in the reciprocal space that are shifted from each other either in momentum or energy. The corresponding chiral structure implies that the time-reversal symmetry or parity is broken. This is also what makes them qualitatively different from the Dirac semimetals, such as A_3Bi ($\text{A} = \text{Na}, \text{K}, \text{Rb}$), Cd_3As_2 , and ZrTe_5 [11–13], in which pairs of opposite-chirality nodes overlap, and both discrete symmetries are preserved.

Formally, the low-energy effective theory of a Weyl semimetal is invariant under the chiral symmetry that is generated by independent phase transformations of the left- and right-handed fermions. Such a symmetry, however, is anomalous in the presence of parallel electric and magnetic fields [14]. In relativistic quantum field theories, the origin of the anomaly is connected with the absence of an ultraviolet (high-energy) regularization consistent with both electric and chiral charge conservation. In condensed matter systems, on the other hand, the Brillouin zone is always finite in the reciprocal space and, thus, ultraviolet divergences are absent. Because of its topological roots [10], however, the chiral anomaly is still present and can have observable implications. One of them is a large negative magnetoresistance [15–18] that was experimentally observed in Na_3Bi [19], Cd_3As_2 [20, 21], ZrTe_5 [22], GdPtBi [23], and TaAs [24].

An efficient approach to study the electromagnetic response of Weyl semimetals is the chiral kinetic theory [25–27], which is the generalization of the standard kinetic theory [28] to the case of Dirac and Weyl quasiparticles. Not only does it capture the topological properties of the chiral fermions via the Berry curvature [29], but also correctly describes the chiral anomaly in background electromagnetic fields. It turns out, however, that the chiral kinetic theory does not include all topological contributions relevant for Weyl semimetals. In particular, it misses the Bardeen-Zumino current (also known as the Chern-Simons current), which is critical for the correct description of the chiral magnetic effect [30, 31], the anomalous Hall effect [32–36], and collective excitations in Weyl materials [37]. Note that the Bardeen-Zumino term [38] was first proposed in relativistic quantum field theories in order to define the consistent anomaly (for an instructive discussion of the Bardeen-Zumino current in the context of Weyl semimetals, see Refs. [39, 40]).

In this connection, let us briefly recall the concepts of covariant and consistent anomalies in the high energy physics [40]. Because of the regularization ambiguity in the calculation of the triangle diagram [14], there is a freedom in the definitions of electric and chiral current densities in quantum field theory with chiral fermions. The results are defined up to a Bardeen-Zumino polynomial [38] in gauge fields. In the covariant scheme, the currents are required to couple covariantly to background gauge fields. However, they cannot be defined as functional variations of a quantum effective action. In the consistent scheme, the corresponding currents are given by the variations of the quantum action. Such currents are consistent with the local electric charge conservation even in the presence of both vector

and axial gauge fields.

Theoretically, the absence of the Bardeen-Zumino current in the chiral kinetic theory becomes a particularly acute problem in Weyl semimetals subjected to pseudoelectromagnetic fields induced by mechanical strains [41–47]. In essence, these fields resemble the ordinary electromagnetic ones, but couple to opposite chirality quasiparticles with different signs. The standard formulation of the chiral kinetic theory would then imply a local nonconservation of the electric charge in background electromagnetic and pseudoelectromagnetic fields. Clearly, this is unacceptable. Therefore, the chiral kinetic theory should be amended by including the additional Bardeen-Zumino terms in the definition of the charge and current densities [37]. In the four-vector notation, the explicit form of the corresponding fermion current reads $j_{\text{BZ}}^\nu = -e^2 \epsilon^{\nu\rho\alpha\beta} A_\rho^5 F_{\alpha\beta} / (4\pi^2)$ [38–40], where field $A_\rho^5 = b_\rho + \tilde{A}_\rho^5$ consists of the strain-induced pseudoelectromagnetic gauge field \tilde{A}_ρ^5 and the chiral shift four-vector $b_\rho = (b_0, -\mathbf{b})$. Note that b_0 and \mathbf{b} describe the energy and momentum-space separation between the Weyl nodes, respectively.

In relativistic field theory, the structure of the Bardeen-Zumino term can be established [38, 39] by requiring that the ultraviolet regularization of the theory is consistent with the electric charge conservation. The same argument is often tacitly followed in Weyl semimetals, although there are no ultraviolet divergencies in condensed matter systems and the concept of chiral quasiparticles works only in the vicinity of the Weyl nodes. Thus, one of the main goals of this study is to understand whether the Bardeen-Zumino current is universal and topologically protected in realistic models of Weyl semimetals with a finite Brillouin zone. As we will show, it is proportional to the winding number of the mapping of a two dimensional section of the Brillouin zone onto the unit sphere and, thus, indeed has a topological origin. Moreover, we will demonstrate that the result is quite general and works even in the case of multi-Weyl semimetals [48–50] (i.e., Weyl semimetals with the topological charge of the nodes greater than one), whose topological responses were recently discussed in Ref. [51] using the Fujikawa’s regularization method.

This paper is organized as follows. In Sec. II, we introduce a generic lattice model of Weyl semimetals and outline the general formalism that we will use to study the electromagnetic response. In Sec. III, we derive the expressions for the electric charge and current densities in the linear order in a background magnetic field and compare the results with their counterparts in the chiral kinetic theory. We study the response to a background electric field in Sec. IV. The response to strain-induced pseudomagnetic and pseudoelectric fields is studied in Secs. V and VI, respectively. The summary of our results and general conclusions are presented in Sec. VII. Technical details of derivations are given in several appendices at the end of the paper. Throughout the paper, we use the units with $\hbar = c = 1$.

II. MODEL

The electron states in a generic lattice Weyl semimetal can be described by the following Hamiltonian [30, 32] in the momentum space:

$$\mathcal{H}_{\text{latt}} = d_0 + \mathbf{d} \cdot \boldsymbol{\sigma}, \quad (1)$$

where $\boldsymbol{\sigma} = (\sigma_1, \sigma_2, \sigma_3)$ are the Pauli matrices and functions d_0 and \mathbf{d} are periodic in quasimomenta $\mathbf{k} = (k_x, k_y, k_z)$. The latter can have, for example, the following explicit form:

$$d_0 = g_0 + g_1 \cos(a_z k_z) + g_2 [\cos(a_x k_x) + \cos(a_y k_y)], \quad (2)$$

$$d_1 = \Lambda \sin(a_x k_x), \quad (3)$$

$$d_2 = \Lambda \sin(a_y k_y), \quad (4)$$

$$d_3 = t_0 + t_1 \cos(a_z k_z) + t_2 [\cos(a_x k_x) + \cos(a_y k_y)], \quad (5)$$

where a_x , a_y , and a_z denote the lattice spacings and parameters g_0 , g_1 , g_2 , Λ , t_0 , t_1 , and t_2 are material dependent. Their characteristic values valid for Na₃Bi are given in Appendix A and will be used in our numerical calculations. Also, for the sake of simplicity, we will assume that the lattice is cubic, i.e., $a_x = a_y = a_z = a$.

As is easy to check, the dispersion relations of quasiparticles described by the model Hamiltonian (1) are given by

$$\epsilon_{\mathbf{k}} = d_0 \pm |\mathbf{d}|. \quad (6)$$

When the parameters are such that $|t_0 + 2t_2| \leq |t_1|$, this model has two Weyl nodes separated in momentum space by $\Delta k_z = 2b_z$, where the chiral shift parameter b_z is given by the following analytical expression:

$$b_z = \frac{1}{a_z} \arccos\left(\frac{-t_0 - 2t_2}{t_1}\right). \quad (7)$$

For simplicity, we will assume that the energy vanishes at the position of Weyl nodes. In terms of the model parameters, this implies that $g_0 + 2g_2 - g_1(t_0 + 2t_2)/t_1 = 0$. In a general case, this condition can be enforced by an appropriate

redefinition of the reference point for the chemical potential. Further, as one can see from the left panel of Fig. 1, d_0 introduces an asymmetry between the valence and conduction bands, which complicates the analysis. Therefore, for the sake of simplicity, in what follows we will drop the term d_0 . It is instructive to note, that ϵ_0 [which is the value of energy (6) at $\mathbf{k} = \mathbf{0}$] defines the height of the “dome” in the energy spectrum. On the other hand, parameter t_1 affects both the momentum space separation between the Weyl nodes and the value of the Fermi velocity.

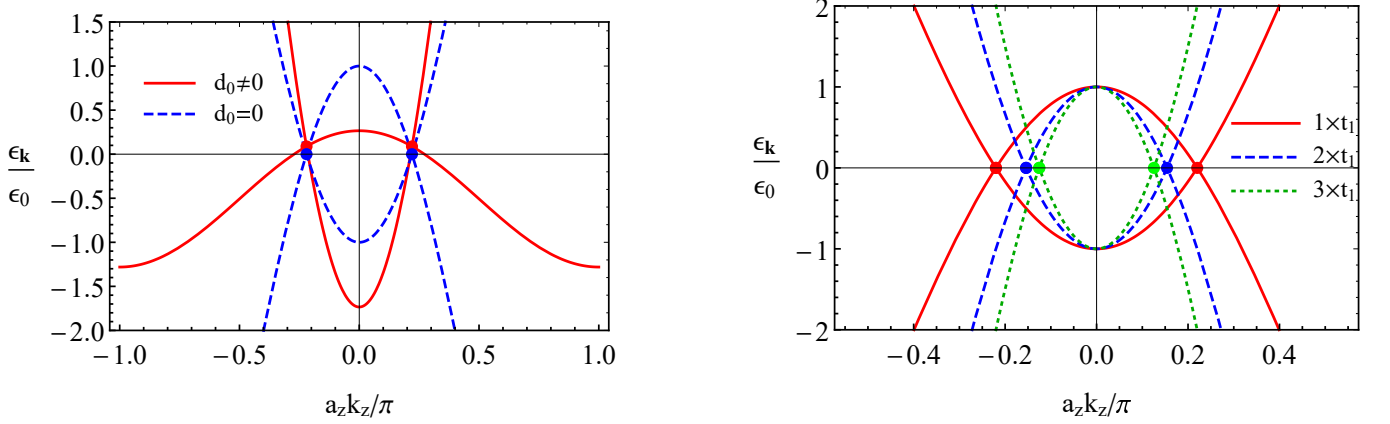


FIG. 1. Left panel: The energy spectrum of the lattice model (1) given by Eq. (6) for $d_0 \neq 0$ (red solid lines) and $d_0 = 0$ (blue dashed lines) as a function of k_z at $k_x = k_y = 0$. Right panel: The energy spectrum (6) for several different values of parameter t_1 . The complete set of model parameters is given in Appendix A.

In order to study a linear electromagnetic response in the Weyl semimetal, we include an interaction with the gauge field through the following interaction term:

$$\mathcal{H}_{\text{int}} = \mathbf{j} \cdot \mathbf{A}, \quad (8)$$

where the electric current density operator in the momentum space is given by

$$\mathbf{j}(\mathbf{k}) = -e \nabla_{\mathbf{k}} \mathcal{H}_{\text{latt}}, \quad (9)$$

and e is a fermion charge. By using Eqs. (2)–(5), we derive the explicit expressions for the components of the current, i.e.,

$$j_x = e a_x [t_2 \sin(k_x a_x) \sigma_z + g_2 \sin(k_x a_x) - \Lambda \cos(k_x a_x) \sigma_x], \quad (10)$$

$$j_y = e a_y [t_2 \sin(k_y a_y) \sigma_z + g_2 \sin(k_y a_y) - \Lambda \cos(k_y a_y) \sigma_y], \quad (11)$$

$$j_z = e a_z [t_1 \sin(k_z a_z) \sigma_z + g_1 \sin(k_z a_z)]. \quad (12)$$

In a many-body system, the electric charge and current densities are given in terms of the quasiparticles Green’s function $G(r, r')$ as follows:

$$\rho = -e \lim_{r' \rightarrow r} \text{tr} [G(r, r')], \quad (13)$$

$$\mathbf{J} = - \lim_{r' \rightarrow r} \text{tr} [\mathbf{j}(-i \nabla_{\mathbf{r}}) G(r, r')], \quad (14)$$

where $r = (t, \mathbf{r})$ and $r' = (t', \mathbf{r}')$. To the linear order in the background electromagnetic fields, the Green’s function has the form

$$G(r, r') = G^{(0)}(r - r') + G^{(1)}(r, r') + \dots \quad (15)$$

Because of translation invariance in the absence of background fields, the zeroth-order Green’s function depends only on the difference $r - r'$. The same is not true, in general, for the first-order part of the Green’s function. The Fourier transform of $G^{(0)}(r - r')$ follows directly from the model Hamiltonian (8), i.e.,

$$G^{(0)}(\omega; \mathbf{k}) = \frac{i [\omega + \mu + (\mathbf{d} \cdot \boldsymbol{\sigma})]}{[\omega + \mu + i0 \text{sgn}(\omega)]^2 - |\mathbf{d}|^2}, \quad (16)$$

where we introduced a nonzero chemical potential μ and omitted d_0 . Now, the correction to the Green's function linear in the electromagnetic field can be obtained by using a perturbative expansion in the interaction Hamiltonian, i.e.,

$$G^{(1)}(r, r') = -i \int dr'' G^{(0)}(r - r'') \mathcal{H}_{\text{int}}(r'') G^{(0)}(r'' - r'). \quad (17)$$

In the next two sections, we will use the above representation for the Green's function in order to study the linear response of Weyl semimetals to background electromagnetic fields. A similar representation, although with a different interaction Hamiltonian, will be also used later in the case of strain-induced pseudoelectromagnetic fields.

III. RESPONSE TO BACKGROUND MAGNETIC FIELD

In this section we derive explicit expressions for the electric charge and current densities to the linear order in a background magnetic field. We assume that the field points in the $+z$ direction and is described by the vector potential in the Landau gauge, i.e., $\mathbf{A} = (0, xB, 0)$. By making use of the definitions in Eqs. (13) and (14), as well as the linear-order correction to the Green's function $G^{(1)}(r, r')$ obtained in Appendix D, we find

$$\rho = \frac{eB}{2} \int \frac{d\omega d^3\mathbf{k}}{(2\pi)^4} \text{tr} \left\{ \left[\partial_{k_x} G^{(0)}(\omega, \mathbf{k}) \right] j_y(\mathbf{k}) G^{(0)}(\omega, \mathbf{k}) - G^{(0)}(\omega, \mathbf{k}) j_y(\mathbf{k}) \left[\partial_{k_x} G^{(0)}(\omega, \mathbf{k}) \right] \right\}, \quad (18)$$

$$J_n = \frac{B}{2} \int \frac{d\omega d^3\mathbf{k}}{(2\pi)^4} \text{tr} \left\{ j_n(\mathbf{k}) \left[\partial_{k_x} G^{(0)}(\omega, \mathbf{k}) \right] j_y(\mathbf{k}) G^{(0)}(\omega, \mathbf{k}) - j_n(\mathbf{k}) G^{(0)}(\omega, \mathbf{k}) j_y(\mathbf{k}) \left[\partial_{k_x} G^{(0)}(\omega, \mathbf{k}) \right] \right. \\ \left. + \delta_{n,x} [\partial_{k_x} j_x(\mathbf{k})] G^{(0)}(\omega, \mathbf{k}) j_y(\mathbf{k}) G^{(0)}(\omega, \mathbf{k}) + 2ix\delta_{n,x} j_x(\mathbf{k}) G^{(0)}(\omega, \mathbf{k}) j_y(\mathbf{k}) G^{(0)}(\omega, \mathbf{k}) \right\}. \quad (19)$$

Note that both densities are given in terms of the zeroth-order Green's function $G^{(0)}(\omega, \mathbf{k})$ defined in Eq. (16), as well as its derivatives with respect to the quasimomentum.

Let us first calculate the electric charge density (18). After substituting the explicit form of the zeroth-order Green's function $G^{(0)}(\omega, \mathbf{k})$, we find that the integration over ω can be performed analytically. For the details of the derivation, see Appendix E 1. In the case of the vanishing chemical potential, the final result reads

$$\rho = -\frac{e^2 B}{2(2\pi)^3} \int d^3\mathbf{k} \left(\hat{\mathbf{d}} \cdot \left[(\partial_{k_x} \hat{\mathbf{d}}) \times (\partial_{k_y} \hat{\mathbf{d}}) \right] \right), \quad (20)$$

where $\hat{\mathbf{d}} \equiv \mathbf{d}/|\mathbf{d}|$. Its topological nature is evident from the fact that the integrand is proportional to the z component of the Berry curvature. Indeed, the latter is defined by [52]

$$\Omega_i = \sum_{l,m=1}^3 \frac{\epsilon_{ilm}}{4} \left(\hat{\mathbf{d}} \cdot \left[(\partial_{k_l} \hat{\mathbf{d}}) \times (\partial_{k_m} \hat{\mathbf{d}}) \right] \right). \quad (21)$$

A component of the Berry curvature can be also viewed as the Jacobian of the mapping of a two dimensional section of the Brillouin zone onto the unit sphere $\hat{\mathbf{k}} \rightarrow \hat{\mathbf{d}}$, i.e., $T^2 \rightarrow S^2$. When integrated over the area of the cross-section (for example, the k_x - k_y plane), it counts the winding number of the mapping, or the Chern number [53]

$$\mathcal{C}(k_z) = \frac{1}{4\pi} \int dk_x dk_y \left(\hat{\mathbf{d}} \cdot \left[(\partial_{k_x} \hat{\mathbf{d}}) \times (\partial_{k_y} \hat{\mathbf{d}}) \right] \right). \quad (22)$$

As is easy to check, $\mathcal{C}(k_z)$ depends on k_z and vanishes for $|k_z| \geq b_z$ in the model under consideration. By integrating the Chern number over k_z , we find that the result for ρ coincides with the topological Bardeen-Zumino expression for the electric charge density induced by a magnetic field [38–40], generalized to the case of a multi-Weyl semimetal, i.e.,

$$\rho_{\text{BZ}} = -n \frac{e^2 B b_z}{2\pi^2}. \quad (23)$$

Here n denotes the topological charge of the Weyl nodes in multi-Weyl semimetals, i.e., $n = 1$ in a Weyl semimetal, $n = 2$ in a double-Weyl semimetal, and $n = 3$ in a triple-one. Indeed, as we show in Appendix B, the corresponding lattice models of multi-Weyl semimetals can be defined by the same Hamiltonian as in Eq. (1), but with a different

choice of functions \mathbf{d} . Then, the electric charge density at $\mu = 0$ will be formally given by the topological expression (20) proportional to the winding number. This finding confirms that the Bardeen-Zumino contribution to the electric charge density is reproduced exactly in lattice models of multi-Weyl semimetals with finite Brillouin zones.

As we already mentioned in the Introduction, the result in Eq. (23) cannot be captured by the chiral kinetic theory. The easiest way to see this is to note that the equations of the chiral kinetic theory do not contain the chiral shift parameter \mathbf{b} at all. It is rather interesting, as we argue below, that the topological Bardeen-Zumino term appears to be the only contribution that the chiral kinetic theory fails to reproduce. In order to fully substantiate this claim, it is instructive to consider the calculation of the electric charge density in the same lattice model at nonzero chemical potential μ .

To the linear order in magnetic field \mathbf{B} , the complete expression for the electric charge density at nonzero chemical potential μ reads

$$\rho = \rho_{\text{BZ}} + \rho_{\mu}, \quad (24)$$

where the additional “matter” part of the density is given by

$$\rho_{\mu} = \frac{e^2 B}{2(2\pi)^3} \int \frac{d^3 \mathbf{k}}{|\mathbf{d}|^3} (\mathbf{d} \cdot [(\partial_{k_x} \mathbf{d}) \times (\partial_{k_y} \mathbf{d})]) \theta(|\mu| - |\mathbf{d}|) + \frac{e^2 B}{(2\pi)^3} \int \frac{d^3 \mathbf{k}}{|\mathbf{d}|} \delta(\mu^2 - |\mathbf{d}|^2) (\mathbf{d} \cdot [(\partial_{k_x} \mathbf{d}) \times (\partial_{k_y} \mathbf{d})]). \quad (25)$$

By making use of the Berry curvature defined in Eq. (21), the matter part can be cast in a simpler form, i.e.,

$$\rho_{\mu} = e^2 \int \frac{d^3 \mathbf{k}}{(2\pi)^3} (\mathbf{B} \cdot \boldsymbol{\Omega}) [\theta(|\mu| - |\mathbf{d}|) + |\mathbf{d}| \delta(|\mu| - |\mathbf{d}|)]. \quad (26)$$

For a specific set of model parameters in Appendix A, it is straightforward to calculate the corresponding contribution to the charge density using numerical methods. It is much more instructive, however, to compare Eq. (26) with its counterpart in the chiral kinetic theory (see, e.g., Ref. [54]):

$$\begin{aligned} \rho_{\text{CKT}} = & \sum_{\eta=\pm} \eta e \int \frac{d^3 \mathbf{k}}{(2\pi)^3} [1 + \eta e(\mathbf{B} \cdot \boldsymbol{\Omega})] \left[1 + e^{(v_F k - e\eta v_F k(\mathbf{B} \cdot \boldsymbol{\Omega}) - \eta\mu)/T} \right] - \sum_{\eta=\pm} \eta e \int \frac{d^3 \mathbf{k}}{(2\pi)^3} n_{\eta}(v_F k) \\ & \simeq \sum_{\eta=\pm} \eta e \int \frac{d^3 \mathbf{k}}{(2\pi)^3} [n_{\eta}(v_F k) + \eta e(\mathbf{B} \cdot \boldsymbol{\Omega}) n_{\eta}(v_F k) - \eta v_F k e(\mathbf{B} \cdot \boldsymbol{\Omega}) n'_{\eta}(v_F k)] - \sum_{\eta=\pm} \eta e \int \frac{d^3 \mathbf{k}}{(2\pi)^3} n_{\eta}(v_F k), \end{aligned} \quad (27)$$

where $n_{\eta}(x) = 1/[1 + e^{(x - \eta\mu)/T}]$ is the Fermi-Dirac distribution, and we set $c = 1$ according to the conventions in this paper. In the zero temperature limit, the corresponding contribution linear in the magnetic field reads

$$\rho_{\text{CKT}} = e^2 \int \frac{d^3 \mathbf{k}}{(2\pi)^3} (\mathbf{B} \cdot \boldsymbol{\Omega}) [\theta(|\mu| - v_F k) + v_F k \delta(|\mu| - v_F k)]. \quad (28)$$

As we see, the chiral kinetic theory result in Eq. (28) reproduces exactly the matter part of the charge density in Eq. (26) obtained in the lattice model of a Weyl semimetal if we set $\mathbf{d} = v_F \mathbf{k}$.

Let us discuss now the electric current density. As in the case of the electric charge density, after substituting the zeroth-order Green's function $G^{(0)}(\omega, \mathbf{k})$, see Eq. (16), into the expression for the current density (19) and performing the integration over ω analytically (see Appendix E1 for details), we obtain

$$J_n = -e^2 B \int \frac{d^3 \mathbf{k}}{(2\pi)^3} \text{sgn}(\mu) \sum_{i,l,m=1}^3 \epsilon_{ilm} (\partial_{k_n} d_i) (\partial_{k_x} d_l) (\partial_{k_y} d_m) \delta(\mu^2 - |\mathbf{d}|^2), \quad (29)$$

where we omitted the imaginary, as well as coordinate-dependent terms that vanish after the integration over the momentum. Further, after integrating over the whole Brillouin zone, we find that the electric current density (29) linear in a constant background magnetic field vanishes. This means that the chiral magnetic effect is absent in the equilibrium state, which is in agreement with general requirements of the band theory of solids [30, 55].

IV. RESPONSE TO BACKGROUND ELECTRIC FIELD

In order to identify the topological Bardeen-Zumino contributions in the electric current density, one needs to study the response of the lattice Weyl model to a background electric field. The corresponding analysis is performed in this section using the Kubo's linear response theory.

In the framework of the Kubo's theory, the charge and current densities can be written in the form $\rho = \sigma_{0m}E_m$ and $J_n = \sigma_{nm}E_m$, respectively. Here $\sigma_{\nu m}$ with $\nu = (0, x, y, z)$ describes the response of the charge and direct current densities to the electric field, which is related to the polarization tensor $\Pi_{\nu m}(\Omega + i0; \mathbf{0})$ via the standard relation:

$$\sigma_{\nu m} = -\lim_{\Omega \rightarrow 0} \frac{i}{\Omega} \Pi_{\nu m}(\Omega + i0; \mathbf{0}), \quad (30)$$

where the polarization tensor is defined in terms of the quasiparticle Green's function, i.e.,

$$\Pi_{\nu m}(\Omega + i0; \mathbf{0}) = -T \sum_{l=-\infty}^{\infty} \int \frac{d^3\mathbf{k}}{(2\pi)^3} \text{tr} \left[j_\nu(\mathbf{k}) G^{(0)}(i\omega_l; \mathbf{k}) j_m(\mathbf{k}) G^{(0)}(i\omega_l - \Omega; \mathbf{k}) \right] \quad (31)$$

and $\omega_l = (2l+1)\pi T$ (with $l \in \mathbb{Z}$) are the fermion Matsubara frequencies. Here, we also introduced the four-vector $j_\nu = (e, -\mathbf{j})$. By following the standard approach, it is convenient to rewrite the Green's function in terms of its spectral function

$$G^{(0)}(i\omega_l; \mathbf{k}) = \int_{-\infty}^{\infty} d\omega \frac{A(\omega; \mathbf{k})}{i\omega_l + \mu - \omega}, \quad (32)$$

where, by definition,

$$A(\omega; \mathbf{k}) \equiv \frac{i}{2\pi} \left[G^{(0)}(\omega + i0; \mathbf{k}) - G^{(0)}(\omega - i0; \mathbf{k}) \right]_{\mu=0} = i \sum_{s=\pm} \frac{|\mathbf{d}| + s(\mathbf{d} \cdot \boldsymbol{\sigma})}{2|\mathbf{d}|} \delta(\omega - s|\mathbf{d}|). \quad (33)$$

As indicated by the delta function, this spectral function describes noninteracting quasiparticles with a vanishing decay width. In realistic models, of course, the corresponding decay width should be nonzero. This can be implemented by using a phenomenological model, in which the delta function is replaced with the Lorentzian distribution, i.e.,

$$\delta_\Gamma(\omega - s|\mathbf{d}|) \equiv \frac{1}{\pi} \frac{\Gamma(\omega)}{(\omega - s|\mathbf{d}|)^2 + \Gamma^2(\omega)}. \quad (34)$$

Note that, at low energies, the quasiparticle width includes a constant part Γ_0 as well as a frequency-dependent part proportional to ω^2 [56], i.e., $\Gamma(\omega) = \Gamma_0(1 + \omega^2/\epsilon_0^2)$. Henceforth, we will omit the argument of Γ . By making use of the spectral representation for the Green's function, Eq. (30) can be recast in the following form:

$$\sigma_{\nu m} = \lim_{\Omega \rightarrow 0} \frac{i}{\Omega} T \sum_{l=-\infty}^{\infty} \int \frac{d^3\mathbf{k}}{(2\pi)^3} \int \int d\omega d\omega' \frac{\text{tr} [j_\nu(\mathbf{k}) A(\omega; \mathbf{k}) j_m(\mathbf{k}) A(\omega'; \mathbf{k})]}{(i\omega_l + \mu - \omega)(i\omega_l - \Omega - i0 + \mu - \omega')}. \quad (35)$$

After performing the summation over the Matsubara frequencies and setting $T = 0$, we derive the following results:

$$\sigma_{0m} = e^2 \pi \int \frac{d^3\mathbf{k}}{(2\pi)^3} \frac{\delta_\Gamma^2(\mu - |\mathbf{d}|) - \delta_\Gamma^2(\mu + |\mathbf{d}|)}{|\mathbf{d}|} (\mathbf{d} \cdot (\partial_{k_m} \mathbf{d})), \quad (36)$$

$$\begin{aligned} \sigma_{nn} = e^2 \pi \int \frac{d^3\mathbf{k}}{(2\pi)^3} \frac{1}{|\mathbf{d}|^2} \Big\{ & ((\partial_{k_n} \mathbf{d}) \cdot \mathbf{d})^2 [\delta_\Gamma^2(\mu - |\mathbf{d}|) + \delta_\Gamma^2(\mu + |\mathbf{d}|)] \\ & - 2\delta_\Gamma(\mu - |\mathbf{d}|)\delta_\Gamma(\mu + |\mathbf{d}|) [((\partial_{k_n} \mathbf{d}) \cdot \mathbf{d})^2 - |\mathbf{d}|^2(\partial_{k_n} \mathbf{d})^2] \Big\}. \end{aligned} \quad (37)$$

In addition, there are also nonzero off-diagonal components of the conductivity tensor. In the clean limit, in particular, the latter read

$$\sigma_{nm} = -\frac{e^2}{2} \int \frac{d^3\mathbf{k}}{(2\pi)^3} \left(\hat{\mathbf{d}} \cdot [(\partial_{k_n} \hat{\mathbf{d}}) \times (\partial_{k_m} \hat{\mathbf{d}})] \right) [1 - \theta(|\mu| - |\mathbf{d}|)], \quad (38)$$

and the only nonvanishing components of this conductivity tensor are $\sigma_{12} = -\sigma_{21}$.

It should be clear that the off-diagonal conductivity σ_{12} in Eq. (38) has a topological origin in the limit of the vanishing chemical potential ($\mu \rightarrow 0$). Indeed, as in the case of the charge density (20), it is determined by the integral of the Chern number (22), or the winding number, which is equal to the topological charge of the Weyl nodes n . After calculating the corresponding integral, we derive the following explicit result for the anomalous Hall conductivity:

$$\sigma_{12} = -\sigma_{21} \stackrel{\mu=0}{=} -n \frac{e^2 b_z}{2\pi^2}. \quad (39)$$

This result corresponds to the expected topological Bardeen-Zumino current that describes the anomalous Hall conductivity [32–36]. For a set of model parameters in Appendix A, the zero-temperature Hall conductivity σ_{12} as a function of the chemical potential μ is plotted in Fig. 2. From a physics viewpoint, the corresponding result includes both the anomalous and matter contributions. It is interesting to note that the total Hall conductivity decreases with increasing the absolute value of chemical potential. Moreover, the corresponding dependence is much steeper in the case of double- and triple-Weyl semimetals. Since the second term with the theta-function in Eq. (38) contains the integration over all filled quasiparticle states, naively it contradicts the conventional wisdom of the Fermi liquid theory which states that the conductivity is related only to the states on the Fermi surface. However, it was shown in Ref. [52] that the corresponding term can be rewritten as a Fermi surface integral and is always present in realistic models at nonzero chemical potential. According to Ref. [57], the off-diagonal conductivity of a completely filled or empty band should be proportional to a primitive reciprocal lattice vector (including zero). Notice that in the model under consideration this requirement is trivially satisfied, because σ_{12} tends to zero when the bands are completely filled or empty ($\mu \rightarrow \pm\infty$).

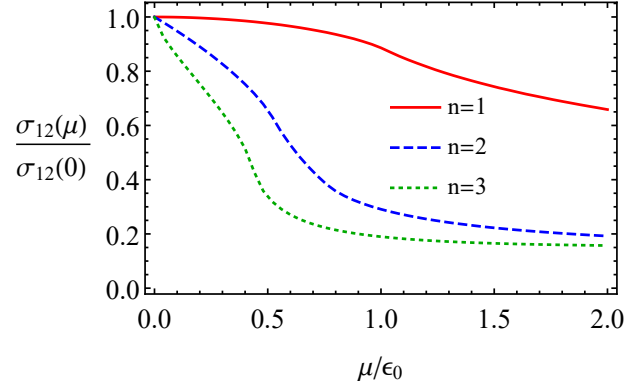


FIG. 2. The dependence of the zero-temperature Hall conductivity σ_{12} in a Weyl semimetal (red solid line), a double-Weyl semimetal (blue dashed line), and a triple Weyl-semimetal (green dotted line) on the chemical potential. Here ϵ_0 is the value of energy (6) at $\mathbf{k} = \mathbf{0}$. The numerical results are calculated for the model parameters in Appendix A.

V. RESPONSE TO A STRAIN-INDUCED PSEUDOMAGNETIC FIELD

In the preceding two sections, we studied the electric charge and current response of a Weyl semimetal to external magnetic and electric fields in the lattice model (1). It is also of interest to investigate the response of Weyl materials to pseudoelectromagnetic fields. The latter, as we mentioned in the Introduction, could be generated by applying mechanical deformations to Weyl semimetals. In this section, we consider the response a Weyl semimetal with $n = 1$ to a strain-induced pseudomagnetic field \mathbf{B}_5 . The response to a pseudoelectric field \mathbf{E}_5 will be studied in the next section.

According to Ref. [46], strains in Weyl materials lead to the following additional terms in Hamiltonian (1):

$$\delta h_{\text{strain}} = \Lambda (u_{13}\sigma_x + u_{23}\sigma_y) \sin(ak_z) - t_1 u_{33}\sigma_z \cos(ak_z), \quad (40)$$

where $u_{ij} = (\partial_i u_j + \partial_j u_i)/2$ is the symmetrized strain tensor and $\mathbf{u} = (u_1, u_2, u_3)$ is the displacement vector. In the vicinity of Weyl nodes, the additional terms given by Eq. (40) can be interpreted as the interaction Hamiltonian of Weyl quasiparticles with the background axial gauge field

$$\mathbf{A}_5 = \frac{1}{ea} \{u_{13} \sin(ab_z), u_{23} \sin(ab_z), u_{33} \cot(ab_z)\}. \quad (41)$$

As is clear, not all strains in Weyl materials can produce nontrivial pseudoelectromagnetic fields. For example, a time independent u_{33} describes a stretching of the crystal along the $+z$ -direction. This leads to a simple redefinition of the parameter $t_1 \rightarrow (1 - u_{33})t_1$ that, in turn, modifies the value of the chiral shift parameter (7). In the rest of this section, we will primarily concentrate on the case of static strains with $\nabla \times \mathbf{A}_5 \neq \mathbf{0}$ that describe pseudomagnetic fields.

We consider the case of a constant strain-induced pseudomagnetic field along the z direction. Such a field can be induced, for example, by applying torsion to a wire made of a Weyl material,

$$\mathbf{B}_5 \equiv \nabla \times \mathbf{A}_5 = -\frac{\theta}{Lea} \sin(ab_z) \hat{\mathbf{z}}, \quad (42)$$

where $\mathbf{u} = \theta z[\mathbf{r} \times \hat{\mathbf{z}}]/L$, θ is the torsion angle, and L is the length of the crystal. Then the interaction Hamiltonian (40) takes the following explicit form:

$$\delta h_{\text{strain}} = \frac{eB_5 a \Lambda \sin(ak_z)}{2 \sin(ab_z)} (x\sigma_y - y\sigma_x). \quad (43)$$

It should be noted that the latter has the same structure as the interaction Hamiltonian in the case of a constant magnetic field \mathbf{B} . This becomes evident by introducing the following notation for the transverse components of the axial current:

$$j_x^5 = \frac{ea\Lambda}{\sin(ab_z)} \sigma_x \sin(ak_z), \quad (44)$$

$$j_y^5 = \frac{ea\Lambda}{\sin(ab_z)} \sigma_y \sin(ak_z). \quad (45)$$

Then, in the full analogy with Eqs. (18) and (19), we derive the following expressions for the electric charge and current densities induced by the pseudomagnetic field:

$$\rho = \frac{eB_5}{4} \int \frac{d\omega d^3\mathbf{k}}{(2\pi)^4} \text{tr} \left\{ -(\partial_{k_y} G^{(0)}) j_x^5 G^{(0)} + G^{(0)} j_x^5 (\partial_{k_y} G^{(0)}) + (\partial_{k_x} G^{(0)}) j_y^5 G^{(0)} - G^{(0)} j_y^5 (\partial_{k_x} G^{(0)}) \right\} \quad (46)$$

$$J_n = \frac{B_5}{4} \int \frac{d\omega d^3\mathbf{k}}{(2\pi)^4} \text{tr} \left\{ -j_n (\partial_{k_y} G^{(0)}) j_x^5 G^{(0)} + j_n G^{(0)} j_x^5 (\partial_{k_y} G^{(0)}) - \delta_{n,y} (\partial_{k_y} j_y) G^{(0)} j_x^5 G^{(0)} - 2iy \delta_{n,y} j_y G^{(0)} j_x^5 G^{(0)} \right. \\ \left. + j_n (\partial_{k_x} G^{(0)}) j_y^5 G^{(0)} - j_n G^{(0)} j_y^5 (\partial_{k_x} G^{(0)}) + \delta_{n,x} (\partial_{k_x} j_x) G^{(0)} j_y^5 G^{(0)} + 2ix \delta_{n,x} j_x G^{(0)} j_y^5 G^{(0)} \right\}, \quad (47)$$

where for the sake of simplicity we dropped the arguments of \mathbf{j} , \mathbf{j}^5 , and $G^{(0)}$. By making use of the integrals in Eqs. (C3)–(C5), we can integrate over ω . Then, by setting $u_{33} = 0$ (see also Appendix E 1), we obtain

$$\rho_{\text{top}} = \frac{e^2 B_5 a \Lambda}{4 \sin(ab_z)} \int \frac{d^3\mathbf{k}}{(2\pi)^3} \frac{\sin(ak_z)}{|\mathbf{d}|^3} \{ [(\partial_{k_y} \mathbf{d}) \times \mathbf{d}]_x - [(\partial_{k_x} \mathbf{d}) \times \mathbf{d}]_y \}, \quad (48)$$

$$\rho_\mu = -\frac{e^2 B_5 a \Lambda}{4 \sin(ab_z)} \int \frac{d^3\mathbf{k}}{(2\pi)^3} \frac{\sin(ak_z)}{|\mathbf{d}|^3} \{ [(\partial_{k_y} \mathbf{d}) \times \mathbf{d}]_x - [(\partial_{k_x} \mathbf{d}) \times \mathbf{d}]_y \} [\theta(|\mu| - |\mathbf{d}|) + |\mathbf{d}| \delta(|\mu| - |\mathbf{d}|)], \quad (49)$$

and

$$J_n = -\frac{e^2 B_5 a \Lambda}{2 \sin(ab_z)} \int \frac{d^3\mathbf{k}}{(2\pi)^3} \sin(ak_z) \text{sgn}(\mu) \delta(\mu^2 - |\mathbf{d}|^2) \left\{ [(\partial_{k_n} \mathbf{d}) \times (\partial_{k_y} \mathbf{d})]_x - [(\partial_{k_n} \mathbf{d}) \times (\partial_{k_x} \mathbf{d})]_y \right\}, \quad (50)$$

where we also omitted imaginary and coordinate dependent terms which vanish after the integration over the whole Brillouin zone. Our numerical calculations show that $\rho_{\text{top}} = \rho_\mu = J_x = J_y = 0$. Thus, unlike the magnetic field considered in Sec. III, the pseudomagnetic field does not induce any electric charge density. On the other hand, the component of electric current along the direction of the pseudomagnetic fields is nonzero. The dependencies of J_z for a Weyl semimetal on the parameters ϵ_0 , t_1 , and chemical potential μ are shown in the left, middle, and right panels of Fig. 3, respectively. In particular, the right panel of Fig. 3 shows that, at sufficiently small values of μ , the electric current agrees with the corresponding expression in the chiral kinetic theory [41, 45],

$$J_{z,\text{CKT}} = -\frac{e^2 \mu B_5}{2\pi^2}. \quad (51)$$

Notably, however, the latter is not exact and receives corrections at large enough values of μ . Also, as we see from the left and middle panels of Fig. 3, the result for the current J_z depends on other model parameters and, consequently, is not fully protected by topology. While this might appear surprising, the reason for this is rather simple and related to the fact that the interpretation of the strain-induced background field (41) as a conventional axial vector potential \mathbf{A}_5 deteriorates outside of the immediate vicinity of the Weyl nodes.

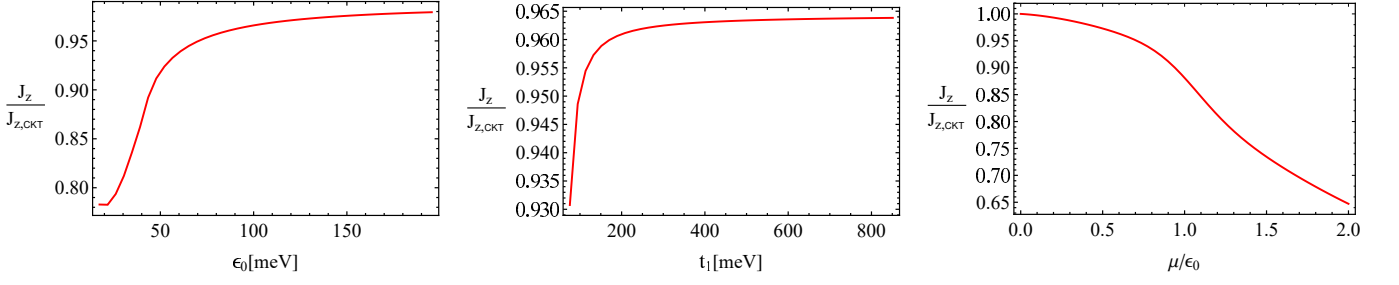


FIG. 3. The electric current density J_z in the direction of the pseudomagnetic field as a function of ϵ_0 (left panel), t_1 (middle panel), and μ/ϵ_0 (right panel). In the left and middle panels, the chemical potential is $\mu = 43.45$ meV. In the middle and right panels, we used $\epsilon_0 = 86.9$ meV, which corresponds to the “dome” energy at $k = 0$ in the model defined in Appendix A.

VI. RESPONSE TO A STRAIN-INDUCED PSEUDOELECTRIC FIELD

In this section, we study the response to a strain-induced pseudoelectric field \mathbf{E}_5 . Such a field can be generated by time-dependent deformations of a Weyl crystal. As in Sec. IV, here we use the Kubo’s linear response theory. By reexpressing the deformation tensor components $u_{ij} \sim t$ in terms of the axial vector potential \mathbf{A}_5 and using the relation $\mathbf{E}_5 = -\partial_t \mathbf{A}_5$, we obtain the following interaction Hamiltonian:

$$\delta h_{\text{strain}} = -\frac{eE_{5,x}a\Lambda \sin(ak_z)}{\sin(ab_z)}\sigma_x t - \frac{eE_{5,y}a\Lambda \sin(ak_z)}{\sin(ab_z)}\sigma_y t + \frac{eE_{5,z}at_1 \cos(ak_z)}{\cot(ab_z)}\sigma_z t. \quad (52)$$

By comparing this with the electromagnetic interaction Hamiltonian (8), we found that the components of the current density operator j_x^5 and j_y^5 are given by Eqs. (44) and (45), respectively, and j_z^5 reads

$$j_z^5 = -e \frac{at_1 \cos(ak_z)}{\cot(ab_z)}\sigma_z. \quad (53)$$

The DC conductivity tensor $\sigma_{\nu m}^{(5)}$ that quantifies the response of the *electric* charge and current densities to a background *pseudoelectric* field \mathbf{E}_5 is given by the standard Kubo’s formula,

$$\sigma_{\nu m}^{(5)} = -\lim_{\Omega \rightarrow 0} \frac{i}{\Omega} \Pi_{\nu m}^{(5)}(\Omega + i0; \mathbf{0}), \quad (54)$$

where the current-current correlator on the right-hand side is defined in terms of the quasiparticle Green’s function as follows:

$$\Pi_{\nu m}^{(5)}(\Omega + i0; \mathbf{0}) = -T \sum_{l=-\infty}^{\infty} \int \frac{d^3 \mathbf{k}}{(2\pi)^3} \text{tr} \left[j_\nu(\mathbf{k}) G^{(0)}(i\omega_l; \mathbf{k}) j_m^5(\mathbf{k}) G^{(0)}(i\omega_l - \Omega; \mathbf{k}) \right]. \quad (55)$$

By following the same method as in Sec. IV, we can express the conductivity in terms of the spectral function,

$$\sigma_{\nu m}^{(5)} = \lim_{\Omega \rightarrow 0} \frac{i}{\Omega} T \sum_{l=-\infty}^{\infty} \int \frac{d^3 \mathbf{k}}{(2\pi)^3} \int \int d\omega d\omega' \frac{\text{tr} [j_\nu(\mathbf{k}) A(\omega; \mathbf{k}) j_m^5(\mathbf{k}) A(\omega'; \mathbf{k})]}{(i\omega_l + \mu - \omega)(i\omega_l - \Omega - i0 + \mu - \omega')}. \quad (56)$$

Then performing the summation over the Matsubara frequencies and setting $T = 0$ at the end, we derive the following result for the dissipative

$$\sigma_{0m}^{(5)} = -e^2 \pi \int \frac{d^3 \mathbf{k}}{(2\pi)^3} \frac{\delta_\Gamma^2(\mu - |\mathbf{d}|) - \delta_\Gamma^2(\mu + |\mathbf{d}|)}{|\mathbf{d}|} d_m \tilde{j}_m^5, \quad (57)$$

$$\begin{aligned} \sigma_{nm}^{(5)} = & -e^2 \pi \int \frac{d^3 \mathbf{k}}{(2\pi)^3} \frac{1}{2|\mathbf{d}|^2} \sum_{s,s'=\pm} \delta_\Gamma(\mu - s|\mathbf{d}|) \delta_\Gamma(\mu - s'|\mathbf{d}|) \left\{ |\mathbf{d}|^2 (\partial_{k_n} d_m) \tilde{j}_m^5 \right. \\ & \left. + ss' \sum_{i_1, i_2, i_3=1}^3 [\delta_{i_1 i_2} \delta_{m i_3} - \delta_{i_1 m} \delta_{i_2 i_3} + \delta_{i_1 i_4} \delta_{i_2 m}] (\partial_{k_n} d_{i_1}) d_{i_2} \tilde{j}_m^5 d_{i_3} \right\}, \end{aligned} \quad (58)$$

as well as nondissipative parts of the conductivity tensor

$$\tilde{\sigma}_{nm}^{(5)} = e \int \frac{d^3\mathbf{k}}{(2\pi)^3} \frac{\tilde{j}_m^5 [\mathbf{d} \times (\partial_{\mathbf{k}_n} \mathbf{d})]_m}{2|\mathbf{d}|^3} [1 - \theta(|\mu| - |\mathbf{d}|)]. \quad (59)$$

Here $\tilde{j}_n^5 = \sum_{m=1}^3 \text{tr}(\sigma_n j_m^5)/2$. Note that in the last equation we explicitly set $\Gamma \rightarrow 0$. Formally, it is similar to the topological off-diagonal components of the conductivity tensor in Eq. (38). Numerically, however, all spatial components vanish after the integration over the whole Brillouin zone.

It is instructive, therefore, to investigate the conductivity tensor in Eqs. (57) and (58) in the case of a nonzero quasiparticle width Γ . The corresponding calculations can be done straightforwardly using numerical methods for a representative set of model parameters in Appendix A. The analysis shows that $\sigma_{03}^{(5)}$ is the only nonzero component of the conductivity tensor. The value of the corresponding component does not appear to be protected by topology. This is clear from its dependence on the chemical potential shown in Fig. 4 for several choices of the quasiparticle width. Note that, by assumption, the transport quasiparticle width includes a constant part Γ_0 as well as a frequency-dependent part proportional to μ^2 [56], i.e., $\Gamma(\mu) = \Gamma_0(1 + \mu^2/\epsilon_0^2)$. We would like to mention also that a nonzero $\sigma_{03}^{(5)}$ is quite interesting from a physics viewpoint. It represents a form of dynamical piezoelectric effect that is driven by time-dependent strains in Weyl metals.

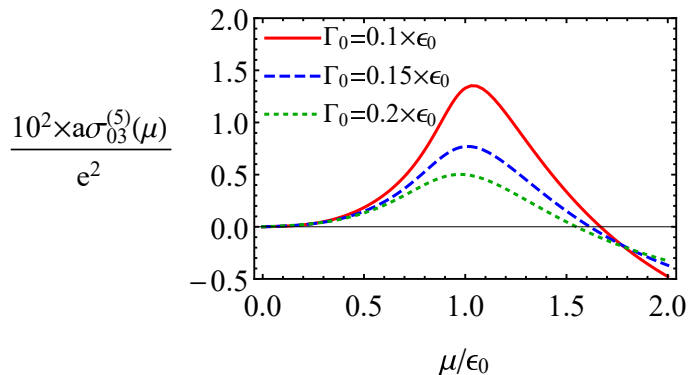


FIG. 4. The dependence of the conductivity tensor component $\sigma_{03}^{(5)}$ on the chemical potential for three different values of the quasiparticle decay width: $\Gamma_0 = 0.1 \epsilon_0$ (red solid line), $\Gamma_0 = 0.15 \epsilon_0$ (blue dashed line), and $\Gamma_0 = 0.2 \epsilon_0$ (green dotted line), respectively. The numerical values of other parameters are defined in Appendix A.

VII. SUMMARY

By making use of a generic lattice model of a Weyl semimetal, we calculated the electric charge and current densities in the first order in background electromagnetic and strain-induced pseudoelectromagnetic fields. A special attention in the analysis was paid to identifying the topological contributions associated with the chiral properties of low-energy quasiparticles. In this connection, it should be mentioned that the key features of the model (including the chiral anomaly) are captured by its topology in the reciprocal space. Unlike the relativistic models in high-energy physics, which are commonly used as a source of intuition for Weyl semimetals, lattice models require no ultraviolet (high-energy) regularization and encounter no ambiguities in predicting physical observables.

Our results for the linear response in background electromagnetic and strain-induced pseudoelectromagnetic fields show that, in addition to the usual matter part, there are two types of topological contributions in the electric charge and current densities. The contributions of the first type are sensitive only to the Berry curvature at Weyl nodes and can be reproduced exactly in the framework of the chiral kinetic theory. The contributions of the second type are determined by a topological invariant (winding number), which is a global property of the whole Brillouin zone, and cannot be captured by the chiral kinetic theory in its standard formulation. Our direct calculations in the lattice model show that the contributions of the second type are given exactly by the Bardeen-Zumino (or, equivalently, Chern-Simons) current. This finding reconfirms, therefore, our claim in Ref. [37] that the physical definition of the electric current in the consistent chiral kinetic theory must be amended by adding the Bardeen-Zumino term.

Our calculations indicate that the linear response in Weyl semimetals in the background pseudoelectromagnetic fields, unlike its counterpart in the electromagnetic fields, is not expected to be completely universal. Indeed, we

found that even the formally topological part of the electric current induced by a constant pseudomagnetic field in Eq. (51) has a nontrivial dependence on the model parameters when the chemical potential is not very small. Such a discrepancy between the naive expectation and the actual calculation can be explained by the fact that the strain-induced fields in Weyl semimetals can be interpreted as the conventional pseudoelectromagnetic fields (i.e., introduced via an axial vector potential \mathbf{A}_5 in the covariant derivatives) only in a close vicinity of the Weyl nodes.

In this paper, we also showed that the same two types of topological currents are also induced in the case of the multi-Weyl semimetals. Our direct calculations reveal, in fact, that the corresponding contributions in the multi-Weyl semimetals contain an additional multiplication factor, which is the integer topological charge of the Weyl nodes. This conclusion is not surprising and, in fact, agrees with a recent independent analysis in Ref. [51], where the high-energy inspired Fujikawa's regularization method was used.

Last but not least, by taking into account the topological origin of the winding number that determines the Bardeen-Zumino terms, our calculation of the current in the lattice model also provides an instructive way of justifying the definition of the consistent electric current in relativistic field theories. Indeed, the formulation of the lattice model itself can be viewed as a form of regularizing a relativistic model that ensures the exact local conservation of the electric charge. In this connection, one should remember, however, that the realization of the chiral symmetry is nontrivial on a lattice [58]. Nevertheless, its implementation as an anomalous symmetry in the low-energy effective theory might be sufficient for most practical purposes.

ACKNOWLEDGMENTS

The work of E.V.G. was partially supported by the Program of Fundamental Research of the Physics and Astronomy Division of the National Academy of Sciences of Ukraine. The work of V.A.M. and P.O.S. was supported by the Natural Sciences and Engineering Research Council of Canada. The work of I.A.S. was supported by the U.S. National Science Foundation under Grant No. PHY-1404232.

Appendix A: Model parameters

In this appendix, we present a representative set of model parameters that we use in our numerical calculations throughout the paper. In order to have a realistic model, we relate the parameters in model (1) to those in Na_3Bi using the parametrization of Ref. [12]. The corresponding relations between the two sets of model parameters read

$$t_0 = M_0 - t_1 - 2t_2, \quad t_{1,2} = -\frac{2M_{1,2}}{a^2}, \quad (\text{A1})$$

$$g_0 = C_0 - g_1 - 2g_2, \quad g_{1,2} = -\frac{2C_{1,2}}{a^2}, \quad (\text{A2})$$

$$\Lambda = \frac{A}{a}, \quad (\text{A3})$$

where the numerical values of the new parameters are fixed by the band structure in Na_3Bi [12],

$$\begin{aligned} C_0 &= -0.06382 \text{ eV}, & C_1 &= 8.7536 \text{ eV } \text{\AA}^2, & C_2 &= -8.4008 \text{ eV } \text{\AA}^2, \\ M_0 &= 0.08686 \text{ eV}, & M_1 &= -10.6424 \text{ eV } \text{\AA}^2, & M_2 &= -10.3610 \text{ eV } \text{\AA}^2, \\ A &= 2.4598 \text{ eV } \text{\AA}. \end{aligned} \quad (\text{A4})$$

For the sake of simplicity, in this paper, we assume that the Weyl semimetal model has a cubic lattice, i.e., $a_x = a_y = a_z = a = 7.5 \text{ \AA}$. Although typically this is not the case in real materials, there are no important topological consequences resulting from such an assumption.

Appendix B: Multi-Weyl semimetals

In this appendix, we discuss how to define a lattice Hamiltonian for multi-Weyl materials by using the same general model as in Eq. (1).

By definition, the multi-Weyl semimetals are Weyl semimetals with the topological charges of Weyl nodes greater than one. The low-energy effective Hamiltonian for the multi-Weyl semimetal can be given in the following form [48–51]:

$$\mathcal{H}_\lambda = \lambda v_F \left[(\mathbf{p} + \lambda \mathbf{b})_3 \sigma_z + (\mathbf{p} + \lambda \mathbf{b})_+^n \sigma_- + (\mathbf{p} + \lambda \mathbf{b})_-^n \sigma_+ \right], \quad (\text{B1})$$

where $n = 2, 3$ is the topological charge of the Weyl nodes, $\lambda = \pm$ is the chirality, $\mathbf{p}_\pm = (p_1 \pm ip_2)/\sqrt{2}$, $\sigma_\pm = (\sigma_x \pm i\sigma_y)/\sqrt{2}$, and \mathbf{b} is the chiral shift parameter that defines the momentum space separation between the Weyl nodes. It is straightforward to check that the corresponding lattice formulation of the Hamiltonian can be given by the same Eq. (1), but with a different choice of functions d_1 and d_2 . In the case of Weyl nodes with the topological charge $n = 2$, for example, one can use the following choice of functions:

$$d_1 = \Lambda \frac{\sin^2(a_x k_x) - \sin^2(a_y k_y)}{\sqrt{2}}, \quad (\text{B2})$$

$$d_2 = \Lambda \frac{\sin(a_x k_x) \sin(a_y k_y)}{\sqrt{2}}. \quad (\text{B3})$$

Similarly, in the case of the Weyl nodes with the topological charge $n = 3$, one can use

$$d_1 = \Lambda \frac{\sin^3(a_x k_x) - 3 \sin(a_x k_x) \sin^2(a_y k_y)}{2}, \quad (\text{B4})$$

$$d_2 = -\Lambda \frac{\sin^3(a_y k_y) - 3 \sin(a_y k_y) \sin^2(a_x k_x)}{2}. \quad (\text{B5})$$

Appendix C: Integrals over ω

In this appendix, we present the results for several types of integrals over ω that we encounter in the calculation of the linear response in the main text, as well as in other appendixes. By omitting the intermediate steps of derivations, here we give only the final results:

$$I_1 = \int \frac{d\omega}{[\omega - d_0 + i0 \operatorname{sgn}(\omega)]^2 - |\mathbf{d}|^2} = -\frac{\pi i}{|\mathbf{d}|} [1 - \theta(|d_0| - |\mathbf{d}|)], \quad (\text{C1})$$

$$I_2 = \int \frac{(\omega - d_0) d\omega}{[\omega - d_0 + i0 \operatorname{sgn}(\omega)]^2 - |\mathbf{d}|^2} = -\pi i \operatorname{sgn}(d_0) \theta(|d_0| - |\mathbf{d}|), \quad (\text{C2})$$

$$I_3 = \int \frac{d\omega}{\left\{[\omega - d_0 + i0 \operatorname{sgn}(\omega)]^2 - |\mathbf{d}|^2\right\}^2} = \frac{\pi i}{|\mathbf{d}|} \left\{ \frac{1}{2|\mathbf{d}|^2} [1 - \theta(|d_0| - |\mathbf{d}|)] - \delta(d_0^2 - |\mathbf{d}|^2) \right\}, \quad (\text{C3})$$

$$I_4 = \int \frac{(\omega - d_0) d\omega}{\left\{[\omega - d_0 + i0 \operatorname{sgn}(\omega)]^2 - |\mathbf{d}|^2\right\}^2} = \pi i \operatorname{sgn}(d_0) [\delta(d_0^2 - |\mathbf{d}|^2) - \delta(-|\mathbf{d}|^2)], \quad (\text{C4})$$

$$I_5 = \int \frac{(\omega - d_0)^2 d\omega}{\left\{[\omega - d_0 + i0 \operatorname{sgn}(\omega)]^2 - |\mathbf{d}|^2\right\}^2} = -\pi i \left\{ \frac{1}{2|\mathbf{d}|} [1 - \theta(|d_0| - |\mathbf{d}|)] + |d_0| \delta(d_0^2 - |\mathbf{d}|^2) \right\}, \quad (\text{C5})$$

where $\theta(x)$ is the unit step function. Note that the above integrals are straightforward to calculate by using the following relations obtained in Ref. [59]:

$$\begin{aligned} \frac{1}{\left\{[\omega - d_0 + i0 \operatorname{sgn}(\omega)]^2 - |\mathbf{d}|^2\right\}^n} &= \frac{1}{\left[(\omega - d_0)^2 - |\mathbf{d}|^2 + i0\right]^n} \\ &\quad + \frac{2\pi i (-1)^{n-1}}{(n-1)!} \theta(|d_0| - |\omega|) \theta(\omega d_0) \delta^{(n-1)}[(\omega - d_0)^2 - |\mathbf{d}|^2], \end{aligned} \quad (\text{C6})$$

$$\begin{aligned} \frac{2n(\omega - d_0)}{\left\{[\omega - d_0 + i0 \operatorname{sgn}(\omega)]^2 - |\mathbf{d}|^2\right\}^{n+1}} &= -\frac{\partial}{\partial \omega} \left(\frac{1}{\left\{[\omega - d_0 + i0 \operatorname{sgn}(\omega)]^2 - |\mathbf{d}|^2\right\}^n} \right) \\ &\quad - \frac{2\pi i (-1)^n}{(n-1)!} \operatorname{sgn}(d_0) \delta^{(n-1)}[(\omega - d_0)^2 - |\mathbf{d}|^2] [\delta(\omega) - \delta(\omega - d_0)]. \end{aligned} \quad (\text{C7})$$

Appendix D: The Green's function in the first order in magnetic field

In this appendix, we present the details of the Green's function calculation in the first order in a constant background magnetic field. Because of the dependence of the vector potential on the spatial coordinate(s), e.g., in the Landau gauge

$A_\nu(\mathbf{r}) = (0, 0, -xB, 0)$, the translation invariance is formally broken and the calculation of the first-order correction to the Green's function $G^{(1)}(r, r')$ becomes rather nontrivial. Indeed, while it is natural to use the momentum-space representation for the translation invariant zeroth-order Green's function, the spatial dependence in the gauge field $A_\nu(\mathbf{r})$ (which enters through the interaction Hamiltonian) complicates the analysis.

In order to partially circumvent the technical complications associated with the absence of translation invariance, it is convenient to utilize the following representation for the spatial coordinate:

$$x'' = \int dp_x \left[-i\partial_{p_x} e^{ip_x x''} \right] \delta(p_x) = \int dp_x e^{ip_x x''} i[\partial_{p_x} \delta(p_x)]. \quad (\text{D1})$$

Then, by using Eq. (17), we can rewrite the first-order correction to the Green's function in the form:

$$G^{(1)}(r, r') = -\frac{B}{2} \int \frac{d\omega d^3\mathbf{k}}{(2\pi)^4} e^{-i\omega(t-t') + i\mathbf{k}(\mathbf{r}-\mathbf{r}')} \left\{ i(x - x') G^{(0)}(\omega, \mathbf{k}) j_y(\mathbf{k}) G^{(0)}(\omega, \mathbf{k}) + 2ix' G^{(0)}(\omega, \mathbf{k}) j_y(\mathbf{k}) G^{(0)}(\omega, \mathbf{k}) \right. \\ \left. + \left[\partial_{k_x} G^{(0)}(\omega, \mathbf{k}) \right] j_y(\mathbf{k}) G^{(0)}(\omega, \mathbf{k}) - G^{(0)}(\omega, \mathbf{k}) j_y(\mathbf{k}) \left[\partial_{k_x} G^{(0)}(\omega, \mathbf{k}) \right] \right\}. \quad (\text{D2})$$

Because of the dependence on the relative coordinate $x - x'$ in the first term in the square brackets, a special care should be taken when using this in the calculation of the current density defined by Eq. (14). Indeed, the definition also contains the current operator $\mathbf{j}(-i\partial_{\mathbf{r}})$ that acts not only on the phase factor $e^{i\mathbf{k}(\mathbf{r}-\mathbf{r}')}$, but also on $(r_n - r'_n)$. The corresponding result can be calculated systematically by using a series representation for the trigonometric functions in the definition of $\mathbf{j}(-i\partial_{\mathbf{r}})$; see Eqs. (10)–(12) with \mathbf{k} replaced by $-i\partial_{\mathbf{r}}$. Thus, by making use of the relations

$$\sin(-ia_n \partial_n) e^{ik_n r_n} \Big|_{r_n \rightarrow 0} = \sum_{m=0}^{\infty} (-1)^n (-ia_n)^{2m+1} \frac{(ik_n)^{2m}}{2m!} = (-ia_n) \cos(a_n k_n), \quad (\text{D3})$$

$$\cos(-ia_n \partial_n) e^{ik_n r_n} \Big|_{r_n \rightarrow 0} = \sum_{m=1}^{\infty} (-1)^n (-ia_n)^{2m} \frac{(ik_n)^{2m-1}}{(2m-1)!} = -(-ia_n) \sin(a_n k_n), \quad (\text{D4})$$

we derive the following result for the current density due to the first term in Eq. (D2):

$$-\frac{B}{2} \lim_{r' \rightarrow r} \int \frac{d\omega d^3\mathbf{k}}{(2\pi)^4} j_n(-i\partial_{\mathbf{r}}) i(r_n - r'_n) G^{(0)}(\omega, \mathbf{k}) j_y(\mathbf{k}) G^{(0)}(\omega, \mathbf{k}) e^{-i\omega(t-t') + i\mathbf{k}(\mathbf{r}-\mathbf{r}')} \\ = -\frac{B}{2} \int \frac{d\omega d^3\mathbf{k}}{(2\pi)^4} (\partial_{k_n} j_n(\mathbf{k})) G^{(0)}(\omega, \mathbf{k}) j_y(\mathbf{k}) G^{(0)}(\omega, \mathbf{k}). \quad (\text{D5})$$

By combining this with the two additional contributions due to the other three terms in the first-order Green's function in Eq. (D2), we will obtain the final result for the current density presented in Eq. (19) in the main text.

Appendix E: Derivation of the electric charge and current densities in background electromagnetic fields

In this appendix, we provide the detailed derivations of the electric charge and current densities in background magnetic and electric fields.

1. Background magnetic field

Let us start with the case of a background magnetic field. The electric charge density in Eq. (18) can be rewritten as follows:

$$\rho = \frac{eB}{2} \int \frac{d\omega d^3\mathbf{k}}{(2\pi)^4} \frac{1}{N^2} \text{tr} \left[(\partial_{k_x} Q) j_y(\mathbf{k}) Q - \frac{1}{N} (\partial_{k_x} N) Q j_y(\mathbf{k}) Q - Q j_y(\mathbf{k}) (\partial_{k_x} Q) + \frac{1}{N} Q j_y(\mathbf{k}) Q (\partial_{k_x} N) \right], \quad (\text{E1})$$

where we used the following shorthand notations for the numerator and denominator of the zeroth-order Green's function $G^{(0)}(\omega, \mathbf{k})$:

$$Q \equiv i[\omega + \mu + (\mathbf{d} \cdot \boldsymbol{\sigma})], \quad (\text{E2})$$

$$N \equiv [\omega + \mu + i0 \text{sgn}(\omega)]^2 - \mathbf{d}^2. \quad (\text{E3})$$

After some algebraic simplifications, this can be rewritten in the following simple form:

$$\rho = \frac{eB}{2} \int \frac{d\omega d^3\mathbf{k}}{(2\pi)^4} \sum_{i_1, i_2, i_3=1}^3 \frac{4i\epsilon_{i_1 i_2 i_3}}{N^2} (\partial_{k_x} d_{i_1}) (\partial_{k_y} d_{i_2}) d_{i_3}. \quad (\text{E4})$$

Finally, performing the integration over ω using the result in Eq. (C3), we obtain the topological and matter parts of the charge density in Eqs. (20) and (26), respectively.

In the case of the electric current density J_n , where $n = 1, 2, 3$, we use the definition in Eq. (19). In the first order in an external magnetic field, it gives

$$J_n = -\frac{e^2 B}{2} \int \frac{d\omega d^3\mathbf{k}}{(2\pi)^4} \frac{1}{N^2} \text{tr} \left\{ (\partial_{k_n} Q)(\partial_{k_x} Q)(\partial_{k_y} Q)Q - (\partial_{k_n} Q)Q(\partial_{k_y} Q)(\partial_{k_x} Q) \right. \\ \left. + \delta_{n,x}(\partial_{k_x}^2 Q)Q(\partial_{k_y} Q)Q + 2irx\delta_{n,x}(\partial_{k_x} Q)Q(\partial_{k_y} Q)Q \right\}. \quad (\text{E5})$$

The first two terms in the curly brackets can be combined to give

$$J_n^{(1)} = -\frac{e^2 B}{2} \int \frac{d\omega d^3\mathbf{k}}{(2\pi)^4} \frac{\omega + \mu}{N^2} \sum_{i_1, i_2, i_3=1}^3 4i\epsilon_{i_1 i_2 i_3} (\partial_{k_n} d_{i_1}) (\partial_{k_x} d_{i_2}) (\partial_{k_y} d_{i_3}). \quad (\text{E6})$$

The last two terms in the curly brackets in Eq. (E5) can be rewritten as follows:

$$J_n^{(2)} = -\delta_{n,x}e^2 B \int \frac{d\omega d^3\mathbf{k}}{(2\pi)^4} \frac{(\omega + \mu)^2}{N^2} [((\partial_{k_x}^2 \mathbf{d}) \cdot (\partial_{k_y} \mathbf{d})) + 2ix((\partial_{k_x} \mathbf{d}) \cdot (\partial_{k_y} \mathbf{d}))] \\ - \delta_{n,x}e^2 B \int \frac{d\omega d^3\mathbf{k}}{(2\pi)^4} \frac{1}{N^2} \sum_{i_1, i_2, i_3, i_4=1}^3 [\delta_{i_1 i_2} \delta_{i_3 i_4} - \delta_{i_1 i_3} \delta_{i_2 i_4} + \delta_{i_1 i_4} \delta_{i_2 i_3}] [(\partial_{k_x}^2 d_{i_1}) + 2ix(\partial_{k_x} d_{i_1})] d_{i_2} (\partial_{k_y} d_{i_3}) d_{i_4}. \quad (\text{E7})$$

Then, we integrate over ω by using Eqs. (C3)–(C5) and arrive at the following result:

$$J_n = -e^2 B \int \frac{d^3\mathbf{k}}{(2\pi)^3} \text{sgn}(\mu) \sum_{i_1, i_2, i_3=1}^3 \epsilon_{i_1 i_2 i_3} (\partial_{k_n} d_{i_1}) (\partial_{k_x} d_{i_2}) (\partial_{k_y} d_{i_3}) \delta(\mu^2 - |\mathbf{d}|^2) \\ + i\delta_{n,x}e^2 B \int \frac{d^3\mathbf{k}}{2(2\pi)^3} [((\partial_{k_x}^2 \mathbf{d}) \cdot (\partial_{k_y} \mathbf{d})) + 2ix((\partial_{k_x} \mathbf{d}) \cdot (\partial_{k_y} \mathbf{d}))] \left\{ \frac{1}{2|\mathbf{d}|} [1 - \theta(|\mu| - |\mathbf{d}|)] + |\mu| \delta(\mu^2 - |\mathbf{d}|^2) \right\} \\ - i\delta_{n,x}e^2 B \int \frac{d^3\mathbf{k}}{2(2\pi)^3} \frac{1}{|\mathbf{d}|} \sum_{i_1, i_2, i_3, i_4=1}^3 [\delta_{i_1 i_2} \delta_{i_3 i_4} - \delta_{i_1 i_3} \delta_{i_2 i_4} + \delta_{i_1 i_4} \delta_{i_2 i_3}] [(\partial_{k_x}^2 d_{i_1}) + 2ix(\partial_{k_x} d_{i_1})] d_{i_2} (\partial_{k_y} d_{i_3}) d_{i_4} \\ \times \left\{ \frac{1}{2|\mathbf{d}|^2} [1 - \theta(|\mu| - |\mathbf{d}|)] - \delta(\mu^2 - |\mathbf{d}|^2) \right\}. \quad (\text{E8})$$

Note that the last two parts vanish after the integration over the whole Brillouin zone.

2. Background electric field

In this subsection we present the details of derivation of the conductivity tensor (35) in Sec. IV. By performing the summation over the Matsubara frequencies in the corresponding expression, we arrive at the conventional representation for the DC conductivity tensor in terms of the spectral function:

$$\sigma_{\nu m} = \text{Re} \left(\lim_{\Omega \rightarrow 0} \frac{i}{\Omega} \int \frac{d^3\mathbf{k}}{(2\pi)^3} \int \int d\omega d\omega' \frac{n_F(\omega) - n_F(\omega')}{\omega - \omega' - \Omega - i0} \text{tr} [j_\nu(\mathbf{k}) A(\omega; \mathbf{k}) \mathbf{j}_m(\mathbf{k}) A(\omega'; \mathbf{k})] \right), \quad (\text{E9})$$

where $n_F(\omega) = 1/[e^{(\omega-\mu)/T} + 1]$ is the Fermi-Dirac distribution, $\nu = 0, 1, 2, 3$, and the spectral function $A(\omega, \mathbf{k})$ is defined in Eq. (33).

In the case of $\nu = 0$, the trace in the expression for the conductivity reads

$$\text{tr} [j_0(\mathbf{k})A(\omega; \mathbf{k})j_m(\mathbf{k})A(\omega'; \mathbf{k})] = \frac{e^2}{2|\mathbf{d}|^2} \sum_{s,s'=\pm} ss' \delta_\Gamma(\omega - s|\mathbf{d}|) \delta_\Gamma(\omega' - s'|\mathbf{d}|) |\mathbf{d}|(s + s') (\mathbf{d} \cdot \partial_{k_m} \mathbf{d}), \quad (\text{E10})$$

where $\delta_\Gamma(x)$ is a regularized form of the δ -function defined in Eq. (34). By substituting this in Eq. (E9), extracting the real part with the help of the Sokhotski formula, and integrating over ω' , we obtain

$$\begin{aligned} \sigma_{0m} &= e^2 \pi \int \frac{d^3 \mathbf{k}}{(2\pi)^3} \int d\omega \frac{1}{4T \cosh^2 \frac{\omega - \mu}{2T}} \frac{1}{2|\mathbf{d}|} \sum_{s,s'=\pm} ss' \delta_\Gamma(\omega - s|\mathbf{d}|) \delta_\Gamma(\omega - s'|\mathbf{d}|) (s + s') (\mathbf{d} \cdot (\partial_{k_m} \mathbf{d})) \\ &\stackrel{T \rightarrow 0}{=} e^2 \pi \int \frac{d^3 \mathbf{k}}{(2\pi)^3} \frac{\delta_\Gamma^2(\mu - |\mathbf{d}|) - \delta_\Gamma^2(\mu + |\mathbf{d}|)}{|\mathbf{d}|} (\mathbf{d} \cdot (\partial_{k_m} \mathbf{d})). \end{aligned} \quad (\text{E11})$$

In the case of $\nu = n$, the result for the trace in Eq. (E9) is given by the following expression:

$$\text{tr} [j_n(\mathbf{k})A(\omega; \mathbf{k})j_m(\mathbf{k})A(\omega'; \mathbf{k})] = -\frac{e^2}{4|\mathbf{d}|^2} \sum_{s,s'=\pm} ss' \delta_\Gamma(\omega - s|\mathbf{d}|) \delta_\Gamma(\omega' - s'|\mathbf{d}|) [i|\mathbf{d}|(s' - s)T_1 + T_2(s, s')], \quad (\text{E12})$$

where we introduced the shorthand notations,

$$T_1 \equiv 2 \sum_{i_1, i_2, i_3=1}^3 \epsilon_{i_1 i_2 i_3} (\partial_{k_n} d_{i_1}) d_{i_2} (\partial_{k_m} d_{i_3}), \quad (\text{E13})$$

$$T_2(s, s') \equiv 2ss'|\mathbf{d}|^2 (\partial_{k_n} \mathbf{d})(\partial_{k_m} \mathbf{d}) + 2 \sum_{i_1, i_2, i_3, i_4=1}^3 [\delta_{i_1 i_2} \delta_{i_3 i_4} - \delta_{i_1 i_3} \delta_{i_2 i_4} + \delta_{i_1 i_4} \delta_{i_2 i_3}] (\partial_{k_n} d_{i_1}) d_{i_2} (\partial_{k_m} d_{i_3}) d_{i_4}. \quad (\text{E14})$$

It is convenient to calculate separately the contributions to the conductivity tensor originating from the two different terms in the square brackets in Eq. (E12). By using the definition in Eq. (E9), we rewrite the contribution due to the first term as follows:

$$\sigma_{nm}^{(1)} = -\text{Re} \left(e^2 \lim_{\Omega \rightarrow 0} \frac{i}{\Omega} \int \frac{d^3 \mathbf{k}}{(2\pi)^3} \int \int d\omega d\omega' \frac{n_F(\omega) - n_F(\omega')}{\omega - \omega' - \Omega} \frac{1}{2|\mathbf{d}|} [\delta_\Gamma(\omega + |\mathbf{d}|) \delta_\Gamma(\omega' - |\mathbf{d}|) - \delta_\Gamma(\omega - |\mathbf{d}|) \delta_\Gamma(\omega' + |\mathbf{d}|)] i T_1 \right). \quad (\text{E15})$$

In order to extract the topological part of the conductivity, we consider the clean limit in Eq. (E15). Thus, by setting $\Gamma \rightarrow 0$ and integrating over ω , we arrive at

$$\sigma_{nm}^{(1)} = e^2 \lim_{\Omega \rightarrow 0} \frac{1}{\Omega} \int \frac{d^3 \mathbf{k}}{(2\pi)^3} \frac{\Omega}{|\mathbf{d}|} [n_F(-|\mathbf{d}|) - n_F(|\mathbf{d}|)] \frac{T_1}{4|\mathbf{d}|^2 - \Omega^2} = e^2 \int \frac{d^3 \mathbf{k}}{(2\pi)^3} \frac{T_1}{4|\mathbf{d}|^3} [n_F(-|\mathbf{d}|) - n_F(|\mathbf{d}|)]. \quad (\text{E16})$$

Taking the limit $T \rightarrow 0$, one can easily obtain Eq. (38).

Similarly, the contribution to the conductivity tensor due to the second term in the square brackets in Eq. (E12) is given by

$$\begin{aligned} \sigma_{nm}^{(2)} &= e^2 \lim_{\Omega \rightarrow 0} \frac{i}{\Omega} \int \frac{d^3 \mathbf{k}}{(2\pi)^3} \int \int d\omega d\omega' [n_F(\omega) - n_F(\omega')] (\pi i) \delta(\omega - \omega' - \Omega) \frac{1}{4|\mathbf{d}|^2} \sum_{s,s'=\pm} ss' \delta_\Gamma(\omega - s|\mathbf{d}|) \delta_\Gamma(\omega' - s'|\mathbf{d}|) \\ &\times T_2(s, s') = e^2 \pi \int \frac{d^3 \mathbf{k}}{(2\pi)^3} \int d\omega \frac{1}{4T \cosh^2 \frac{\omega - \mu}{2T}} \frac{1}{4|\mathbf{d}|^2} \sum_{s,s'=\pm} ss' \delta_\Gamma(\omega - s|\mathbf{d}|) \delta_\Gamma(\omega - s'|\mathbf{d}|) T_2(s, s'). \end{aligned} \quad (\text{E17})$$

After integrating over ω and taking the limit $T \rightarrow 0$, the above expression reduces to Eq. (37).

-
- [1] X. Wan, A. M. Turner, A. Vishwanath, and S. Y. Savrasov, Phys. Rev. B **83**, 205101 (2011).
 [2] H. M. Weng, C. Fang, Z. Fang, B. A. Bernevig, and X. Dai, Phys. Rev. X **5**, 011029 (2015).

- [3] B. Q. Lv, H. M. Weng, B. B. Fu, X. P. Wang, H. Miao, J. Ma, P. Richard, X. C. Huang, L. X. Zhao, G. F. Chen, Z. Fang, X. Dai, T. Qian, and H. Ding, *Phys. Rev. X* **5**, 031013 (2015).
- [4] X. Huang, L. Zhao, Y. Long, P. Wang, D. Chen, Z. Yang, H. Liang, M. Xue, H. Weng, Z. Fang, X. Dai, and G. Chen, *Phys. Rev. X* **5**, 031023 (2015).
- [5] S.-Y. Xu, I. Belopolski, N. Alidoust, M. Neupane, G. Bian, C. Zhang, R. Sankar, G. Chang, Z. Yuan, C.-C. Lee, S.-M. Huang, H. Zheng, J. Ma, D. S. Sanchez, B. Wang, A. Bansil, F. Chou, P. P. Shibayev, H. Lin, S. Jia, and M. Z. Hasan, *Science* **349**, 613 (2015).
- [6] S.-M. Huang, S.-Y. Xu, I. Belopolski, C.-C. Lee, G. Chang, B. Wang, N. Alidoust, G. Bian, M. Neupane, C. Zhang, S. Jia, A. Bansil, H. Lin, and M. Z. Hasan *Nat. Commun.* **6**, 7373 (2015).
- [7] C.-L. Zhang, S.-Y. Xu, I. Belopolski, Z. Yuan, Z. Lin, B. Tong, G. Bian, N. Alidoust, C.-C. Lee, S.-M. Huang, T.-R. Chang, G. Chang, C.-H. Hsu, H.-T. Jeng, M. Neupane, D. S. Sanchez, H. Zheng, J. Wang, H. Lin, C. Zhang, H.-Z. Lu, S.-Q. Shen, T. Neupert, M. Z. Hasan, and S. Jia, *Nat. Commun.* **7**, 10735 (2016).
- [8] S. Borisenko, D. Evtushinsky, Q. Gibson, A. Yaresko, T. Kim, M. N. Ali, B. Buechner, M. Hoesch, and R. J. Cava, *arXiv:1507.04847*.
- [9] I. Belopolski, S.-Y. Xu, Y. Ishida, X. Pan, P. Yu, D. S. Sanchez, M. Neupane, N. Alidoust, G. Chang, T.-R. Chang, Y. Wu, G. Bian, H. Zheng, S.-M. Huang, C.-C. Lee, D. Mou, L. Huang, Y. Song, B. Wang, G. Wang, Y.-W. Yeh, N. Yao, J. Rault, P. Lefevre, F. Bertran, H.-T. Jeng, T. Kondo, A. Kaminski, H. Lin, Z. Liu, F. Song, S. Shin, and M. Z. Hasan, *arXiv:1512.09099*.
- [10] H. B. Nielsen and M. Ninomiya, *Nucl. Phys. B* **185**, 20 (1981); **193**, 173 (1981); **195**, 541 (1982).
- [11] Z. Wang, H. Weng, Q. Wu, X. Dai, and Z. Fang, *Phys. Rev. B* **88**, 125427 (2013).
- [12] Z. Wang, Y. Sun, X. Q. Chen, C. Franchini, G. Xu, H. Weng, X. Dai, and Z. Fang, *Phys. Rev. B* **85**, 195320 (2012).
- [13] H. Weng, X. Dai, and Z. Fang, *Phys. Rev. X* **4**, 011002 (2014).
- [14] S. L. Adler, *Phys. Rev.* **177**, 2426 (1969); J. S. Bell and R. Jackiw, *Nuovo Cim. A* **60**, 47 (1969).
- [15] V. Aji, *Phys. Rev. B* **85**, 241101 (2012).
- [16] D. T. Son and B. Z. Spivak, *Phys. Rev. B* **88**, 104412 (2013).
- [17] E. V. Gorbar, V. A. Miransky, and I. A. Shovkovy, *Phys. Rev. B* **89**, 085126 (2014).
- [18] A. A. Burkov, *Phys. Rev. B* **91**, 245157 (2015).
- [19] J. Xiong, S. K. Kushwaha, T. Liang, J. W. Krizan, M. Hirschberger, W. Wang, R. J. Cava, and N. P. Ong, *Science* **350**, 413 (2015).
- [20] C.-Z. Li, L.-X. Wang, H. Liu, J. Wang, Z.-M. Liao, and D.-P. Yu, *Nat. Commun.* **6**, 10137 (2015).
- [21] H. Li, H. He, H.-Z. Lu, H. Zhang, H. Liu, R. Ma, Z. Fan, S.-Q. Shen, and J. Wang, *Nat. Commun.* **7**, 10301 (2016).
- [22] Q. Li, D. E. Kharzeev, C. Zhang, Y. Huang, I. Pletikoscic, A. V. Fedorov, R. D. Zhong, J. A. Schneeloch, G. D. Gu, and T. Valla, *Nature Phys.* **12**, 550 (2016).
- [23] M. Hirschberger, S. Kushwaha, Z. Wang, Q. Gibson, S. Liang, C.A. Belvin, B. A. Bernevig, R. J. Cava, and N. P. Ong, *Nature Materials* **15**, 1161 (2016).
- [24] C.-L. Zhang, S.-Y. Xu, I. Belopolski, Z. Yuan, Z. Lin, B. Tong, G. Bian, N. Alidoust, C.-C. Lee, S.-M. Huang, T.-R. Chang, G. Chang, C.-H. Hsu, H.-T. Jeng, M. Neupane, D.S. Sanchez, H. Zheng, J. Wang, H. Lin, C. Zhang, H.-Z. Lu, S.-Q. Shen, T. Neupert, M. Z. Hasan, and S. Jia, *Nature Comm.* **7**, 10735 (2016).
- [25] D. T. Son and N. Yamamoto, *Phys. Rev. Lett.* **109**, 181602 (2012).
- [26] M. A. Stephanov and Y. Yin, *Phys. Rev. Lett.* **109**, 162001 (2012).
- [27] D. T. Son and N. Yamamoto, *Phys. Rev. D* **87**, 085016 (2013).
- [28] E. M. Lifshitz and L. P. Pitaevskii, *Physical kinetics* (Pergamon Press, New York, 1981).
- [29] M. V. Berry, *Proc. R. Soc. London, Ser. A* **392**, 45 (1984).
- [30] M. M. Vazifeh and M. Franz, *Phys. Rev. Lett.* **111**, 027201 (2013).
- [31] G. Basar, D. E. Kharzeev, and H. U. Yee, *Phys. Rev. B* **89**, 035142 (2014).
- [32] K.-Y. Yang, Y.-M. Lu, and Y. Ran, *Phys. Rev. B* **84**, 075129 (2011).
- [33] A. A. Burkov and L. Balents, *Phys. Rev. Lett.* **107**, 127205 (2011).
- [34] A. G. Grushin, *Phys. Rev. D* **86**, 045001 (2012).
- [35] A. A. Zyuzin and A. A. Burkov, *Phys. Rev. B* **86**, 115133 (2012).
- [36] P. Goswami and S. Tewari, *Phys. Rev. B* **88**, 245107 (2013).
- [37] E. V. Gorbar, V. A. Miransky, I. A. Shovkovy, and P. O. Sukhachov, *Phys. Rev. Lett.* **118**, 127601 (2017); *Phys. Rev. B* **95**, 115202 (2017); **95**, 115422 (2017).
- [38] W. A. Bardeen, *Phys. Rev.* **184**, 1848 (1969); W. A. Bardeen and B. Zumino, *Nucl. Phys. B* **244**, 421 (1984).
- [39] K. Landsteiner, *Phys. Rev. B* **89**, 075124 (2014).
- [40] K. Landsteiner, *Acta Phys. Polonica B* **47**, 2617 (2016).
- [41] J. Zhou, H. Jiang, Q. Niu, and J. Shi, *Chin. Phys. Lett.* **30**, 027101 (2013).
- [42] M. A. Zubkov, *Annals Phys.* **360**, 655 (2015).
- [43] A. Cortijo, Y. Ferreira, K. Landsteiner, and M. A. H. Vozmediano, *Phys. Rev. Lett.* **115**, 177202 (2015).
- [44] A. Cortijo, D. Kharzeev, K. Landsteiner, and M. A. H. Vozmediano, *Phys. Rev. B* **94**, 241405 (2016).
- [45] A. G. Grushin, J. W. F. Venderbos, A. Vishwanath, and R. Ilan, *Phys. Rev. X* **6**, 041046 (2016).
- [46] D. I. Pikulin, A. Chen, and M. Franz, *Phys. Rev. X* **6**, 041021 (2016).
- [47] T. Liu, D. I. Pikulin, and M. Franz, *Phys. Rev. B* **95**, 041201 (2017).
- [48] G. Volovik and V. Konyshov, *JETP Lett.* **47**, 250 (1988).
- [49] C. Fang, M. J. Gilbert, X. Dai, and B. A. Bernevig, *Phys. Rev. Lett.* **108**, 266802 (2012).

- [50] X. Li, B. Roy, and S. Das Sarma, Phys. Rev. B **94**, 195144 (2016).
- [51] Z.-M. Huang, J. Zhou, and S.-Q. Shen, arXiv:1705.04576.
- [52] F. D. M. Haldane, Phys. Rev. Lett. **93**, 206602 (2004).
- [53] B. A. Bernevig, *Topological insulators and topological superconductors* (Princeton University Press, Princeton, 2013).
- [54] E. V. Gorbar, V. A. Miransky, I. A. Shovkovy, and P. O. Sukhachov, Phys. Rev. B **95**, 205141 (2017).
- [55] N. W. Ashcroft and N. D. Mermin, *Solid state physics* (Saunders College, Philadelphia, 1976).
- [56] A. A. Burkov, M. D. Hook, and L. Balents, Phys. Rev. B **84**, 235126 (2011).
- [57] M. Kohmoto, B. I. Halperin, and Y.-S. Wu, Phys. Rev. B **45**, 13488 (1992).
- [58] P. H. Ginsparg and K. G. Wilson, Phys. Rev. D **25**, 2649 (1982).
- [59] E. V. Gorbar, V. A. Miransky, I. A. Shovkovy, and X. Wang, Phys. Rev. D **88**, 025025 (2013).